Published in final edited form as:
Biochem Pharmacol. 2012 January 1; 83(1): 16–26. doi:10.1016/j.bcp.2011.09.017.

MG-2477, a new tubulin inhibitor, induces autophagy through inhibition of the Akt/mTOR pathway and delayed apoptosis in A549 cells

Giampietro Viola[a,1,*], **Roberta Bortolozzi**[a,1], **Ernest Hamel**[b], **Stefano Moro**[c], **Paola Brun**[d], **Ignazio Castagliuolo**[d], **Maria Grazia Ferlin**[c], and **Giuseppe Basso**[a]

[a]Department of Pediatrics, Laboratory of Oncohematology, University of Padova, Italy

[b]Screening Technologies Branch, Developmental Therapeutics Program, Division of Cancer Treatment and Diagnosis, National Cancer Institute at Frederick, National Institutes of Health, Frederick, MD 21702, USA

[c]Department of Pharmaceutical Sciences, University of Padova, Italy

[d]Department of Histology, Microbiology and Medical Biotechnologie, University of Padova, Italy

Abstract

We previously demonstrated that MG-2477 (3-cyclopropylmethyl-7-phenyl-3*H*-pyrrolo[3,2-*f*]quinolin-9(6*H*)-one) inhibits the growth of several cancer cell lines *in vitro*. Here we show that MG-2477 inhibited tubulin polymerization and caused cells to arrest in metaphase. The detailed mechanism of action of MG-2477 was investigated in a non-small cell lung carcinoma cell line (A549). Treatment of A549 cells with MG-2477 caused the cells to arrest in the G2/M phase of the cell cycle, with a concomitant accumulation of cyclin B. Moreover, the compound induced autophagy, which was followed at later times by apoptotic cell death. Autophagy was detected as early as 12 h by the conversion of microtubule associated protein 1 light chain 3 (LC3-I) to LC3-II, following cleavage and lipid addition to LC3-I. After 48 h of MG-2477 exposure, phosphatidylserine externalization on the cell membrane, caspase-3 activation, and PARP cleavage occurred, revealing that apoptotic cell death had begun. Pharmacological inhibition of autophagy with 3-methyladenine or bafilomycin A1 increased apoptotic cell death, suggesting that the autophagy caused by MG-2477 played a protective role and delayed apoptotic cell death. Additional studies revealed that MG-2477 inhibited survival signaling by blocking activation of Akt and its downstream targets, including mTOR, and FHKR. Treatment with MG-2477 also reduced phosphorylation of mTOR downstream targets p70 ribosomal S6 kinase and 4E-BP1. Overexpression of Akt by transfection with a Myr-Akt vector decreased MG-2477 induced autophagy, indicating that Akt is involved. Taken together, these results indicated that the autophagy induced by MG-2477 delayed apoptosis by exerting an adaptive response following microtubule damage.

Keywords

Autophagy; Apoptosis; Microtubule inhibitors; Cell cycle analysis; Akt/mTOR

[*]Corresponding author. Tel.: +39 049 8211451; fax: +39 049 8211462. giampietro.viola.1@unipd.it (G. Viola).
[1]These authors contributed equally to this work.

Conflict of interest statement
The authors declare that there are no conflicts of interest.

1. Introduction

Antimitotic agents, primarily of natural origin, are a class of compounds that have been used for the treatment of a variety of malignancies for many years. Although they are sometimes considered “old chemotherapeutics” with respect to current anticancer approaches [1,2], at the present time they still represent valuable drugs that retain high scientific interest. Their impressive success in patients is due to their potent antiproliferative effects and to their particular mechanism of action of altering microtubule dynamics, whether their detailed mechanism of action involves inhibition of tubulin assembly (vinca alkaloids, eribulin, estramustine) or inhibition of microtubule disassembly (taxoids, epothilones). The importance of microtubules in mitosis and cell division, as well as the clinical success of microtubule targeting drugs, has made these dynamic organelles one of the most attractive targets for anticancer therapy [3].

As with many anticancer drugs, the mode of action of antitubulin agents involves the induction of programmed cell death (PCD) [4]. Apoptosis (Type I PCD) is characterized by chromatin condensation, DNA fragmentation and activation of caspases. In recent years, it became evident that other forms of cell death, alternatives to apoptosis, are also “programmed”. Among them, autophagy (Type II PCD) is now recognized as an important process involved in different human pathologies, such as neurodegenerative diseases, aging and cancer [5,6]. Recent studies have suggested that, like apoptosis, autophagy is important in the regulation of cancer development and progression and in determining the response of tumor cells to anticancer therapy. In fact, autophagy has been observed as a novel response to some anticancer agents, such as temozolomide, dexamethasone, 6-thioguanine, and camptothecin, as well as to ionizing radiation [7–11]. In this context, very few studies report the possibility that antimitotic drugs might induce autophagy [12–14]. From a molecular point of view, several cell signaling pathways have been implicated in regulating autophagy, including phosphatidyl inositol 3-kinase (PI3K)/Akt/mammalian target of rapamycin (mTOR). Recent studies have shown that the inhibition of Akt and its downstream target mTOR contribute to the initiation of autophagy [15,16].

Recently, we identified MG-2477 (3-cyclopropylmethyl-7-phenyl-3*H*-pyrrolo[3,2-*f*]quinolin-9(6*H*)-one) (structure shown in Fig. 1, Panel A), as a potent growth inhibitor of human tumor cell lines that might interfere with microtubules [17]. The current investigation was designed to characterize the action of MG-2477 in a human tumor cell line (A549 non-small cell lung carcinoma cells) and to characterize the molecular mechanisms by which MG-2477 caused cell death. We focused our attention on this cell line due to the poor prognosis and lack of effective therapies in treating lung carcinoma patients. We show here that MG-2477 was a potent cytotoxic antimicrotubule agent that induced autophagy in A549 cells. Autophagy was followed by apoptotic cell death that was caspase-dependent but did not involve mitochondrial dysfunction.

2. Materials and methods

2.1. Chemicals

3-Cyclopropylmethyl-7-phenylpyrrolo[3,2-*f*]quinolinone, abbreviated MG-2477, was synthesized at the Department of Pharmaceutical Sciences, University of Padova, Italy, as previously described [17]. 3-Methyladenine (3-MA), *N*-benzyloxycarbonyl-Val-Ala-DL-Asp-fluoromethylketone (z-VAD.fmk), *N*-benzyloxycarbonyl-Val-Asp-Val-Ala-Asp-fluoromethylketone (z-VDVAD.fmk) and bafilomycin A1 were purchased from Sigma–Aldrich (Milano, Italy), *N*-benzyloxycarbonyl-Leu-Glu-His-Asp-fluoromethylketone (z-LEHD.fmk), was purchased from Vinci-Biochem (Vinci, Italy).

2.2. Cell lines and growth inhibition assay

The human non-small cell lung carcinoma (A549) cell line was purchased from the American Type Culture Collection. The cells were grown in Dulbecco's modified Eagle's medium (Invitrogen, Milano, Italy), supplemented with 10% heat-inactivated fetal bovine serum, 100 U/mL penicillin G and 10 μg/mL streptomycin at 37 °C in a humidified incubator with 5% CO_2.

The cytotoxic activity of MG-2477 was determined using a standard 3-[4,5-dimethylthiazol-2-yl]-2,5-diphenyltetrazodium bromide (MTT) based colorimetric assay (Sigma–Aldrich, Milano, Italy). Briefly, A549 cells were seeded at a density of 8×10^3 cells/well in 96-well microtiter plates. After 24 h, cells were exposed to the test compound. After different times, cell survival was determined by the addition of an MTT solution as described previously [18].

2.3. In vitro microtubule assembly assay and colchicine binding to tubulin

To evaluate the effect of MG-2477 on tubulin assembly *in vitro*, varying concentrations were preincubated with 10 μM tubulin in glutamate buffer at 30 °C and then cooled to 0 °C. After addition of GTP, the mixtures were transferred to 0 °C cuvettes in a recording spectrophotometer and warmed to 30 °C, and the assembly of tubulin was observed turbidimetrically at 350 nm. The IC_{50} was defined as the compound concentration that inhibited the extent of assembly by 50% after a 20 min incubation [19]. The capacity of compound MG-2477 to inhibit colchicine binding to tubulin was measured as described [20], except that the reaction mixtures contained 1 μM tubulin, 5 μM [^{3}H]colchicine (New England Nuclear, Boston, MA) and 1 μM test compound.

2.4. Mitotic index determination

A549 cells were incubated with MG-2477 for 12 and 24 h prior to centrifugation, and the cell pellet was resuspended in 10 mL of 75 mM KCl at room temperature. After 10 min, 1 mL of methanol–acetic acid (3:l) as fixative was slowly added with mild agitation of the mixture.

Slides were prepared after cells were repelleted, washed twice with 10 mL of the fixative, and resuspended in fixative. After drying, samples were stained with Giemsa solution. Two hundred cells/treatment were scored for the presence of mitotic figures by optical microscopy, and the mitotic index was calculated as the proportion of cells with mitotic figures.

2.5. Molecular docking simulations-target structures

Tubulin complexed with colchicine was retrieved from the PDB (PDB code: 1SA0) [21]. Hydrogen atoms were added, using standard geometries, to the protein structure with the Molecular Operation Environment (MOE, version 2009.10) program [22].

2.6. Molecular docking protocol

MG-2477 was built using the "Builder" module of MOE, and it was docked into the putative colchicine site using flexible MOE-Dock methodology. The purpose of MOE-Dock is to search for favorable binding configurations between a small, flexible ligand and a rigid macromolecular target. Searching is conducted within a user-specified 3D docking box, using the "tabù search" protocol [23] and the MMFF94 force field [24]. Charges for ligands were imported from the MOPAC program [25] output files. MOE-Dock performs a user-specified number of independent docking runs (50 in the present case) and writes the resulting conformations and their energies to a molecular database file. The resulting

MG-2477/tubulin complexes were subjected to MMFF94 all-atom energy minimization until the *rms* of the conjugate gradient was <0.1 kcal mol^{-1} $Å^{-1}$. GB/SA approximation [26] was used to model the electrostatic contribution to the free energy of solvation in a continuum solvent model. The interaction energy values were calculated as the energy of the complex minus the energy of the ligand minus the energy of tubulin: $\Delta E_{inter} = E_{(complex)} - (E_{(L)} + E_{(Tubulin)})$.

2.7. Immunocytochemistry

A549 cells (5×10^3/well) were seeded on chamber slides. After 24 h, MG-2477 (0.1–1 μM) was added to the culture medium, and cells were incubated for a further 24–48 h. As described previously [27], cells were fixed in cold 4% paraformaldehyde for 15 min, rinsed and stored prior to analysis. Primary antibody staining was performed for β-tubulin (Millipore, Billerica, MA). After incubation, cells were washed and incubated with a secondary antibody conjugated to Alexa Fluor 594 (1:2000, Invitrogen, Milano, Italy). Cells were counterstained with 4′,6-diamidino-2-phenylindole (DAPI) (Sigma–Aldrich, Milano, Italy). Cells were examined by fluorescence microscopy (Nikon Eclipse 80i, Melville, NY, USA).

2.8. Externalization of phosphatidylserine (PS)

Surface exposure of phosphatidylserine (PS) by apoptotic cells was measured by flow cytometry with a Coulter Cytomics FC500 (Beckmann Coulter, USA) instrument by adding Annexin-V-FITC to cells according to the manufacturer's instructions (Annexin-V Fluos, Roche Diagnostic, Monza, Italy). Simultaneously, the cells were stained with propidium iodide (PI).

2.9. Analysis of cell cycle distribution

5×10^5 A549 cells in exponential growth were treated with different concentrations of MG-2477 for different times. After the incubation, cells were collected, centrifuged and fixed with ice-cold ethanol (70%) and analyzed as described previously [18].

2.10. Assessment of mitochondrial changes and release of cytochrome c

The mitochondrial membrane potential was measured with the lipophilic cation 5,5′,6,6′-tetrachlo-1,1′,3,3′-tetraethylbenzimidazol-carbocyanine (JC-1, Molecular Probes, Eugene, OR, USA), while the production of reactive oxygen species (ROS) was followed by flow cytometry using the fluorescent dyes hydroethidine (HE, Molecular Probes, Eugene, OR, USA) and 2′,7′-dichlorodihydro-fluorescein diacetate (H_2DCFDA, Molecular Probes, Eugene, OR, USA), as previously described [18]. Cytochrome *c* release was analyzed by immunocytochemistry using a commercial kit (Innocyte flow cytometric cytochrome *c* release kit, from Calbiochem, Milano, Italy) following the manufacturer's instructions.

2.11. Flow cytometric analysis of caspase-3

Caspase-3 activation in A549 cells was evaluated by flow cytometry using a human active caspase-3 fragment antibody conjugated to FITC (BD Biosciences, Milano, Italy). Briefly, after treatment, the cells were collected by centrifugation and resuspended in Perm/Wash™ (BD Biosciences, Milano, Italy) buffer for 20 min, washed and then incubated for 30 min with the antibody. After this period, the cells were washed and analyzed by flow cytometry.

2.12. Examination of LC3 translocation

A549 cells were cultured on 6 well plates in a complete medium for 24 h. Cells were transfected with green fluorescent protein labeled LC3 (GFP-LC3) using Effectene Transfection Reagent (Qiagen, Milano, Italy) and incubated for another 24 h to permit

expression of the GFP-LC3 fusion protein. The localization of LC3 in transfected cells after treatment with MG-2477 was determined by fluorescence microscopy.

2.13. Detection of acidic vesicular organelles (AVOs) and autophagic vacuoles

To detect and quantitate acidic vesicular organelles (AVOs) in treated cells, we performed flow cytometric analysis of acridine orange (AO, Molecular Probes, Eugene, OR, USA) stained cells as described [10]. The formation of AVOs was also visualized by confocal microscopy. Briefly, at the appropriate time points following treatment with MG-2477, cells were incubated for 15 min with medium containing 0.5 μg/mL of AO. The AO was removed, and fluorescent micrographs were taken with a video confocal microscope (Nikon Eclipse 80i, Melville, NY, USA), using a Nikon Nir Apo 60×/1.0W water immersion objective. Autophagic vacuoles were detected with monodansylcadaverine (MDC, Invitrogen Milano, Italy). After incubation of the cells with MG-2477, cells were incubated with MDC (50 μM) in HBSS at 37 °C for 15 min, then washed, and micrographs were prepared as described above.

2.14. Western blot analysis

Cells were treated with MG-2477 and, after different times, were collected, centrifuged and washed two times with ice cold phosphate-buffered saline (PBS). The pellet was then resuspended in lysis buffer as described [27]. The protein concentration in the supernatant was determined using the BCA protein assay (Pierce, Milano, Italy). Equal amounts of protein (10–20 μg) were resolved using SDS-PAGE gel electrophoresis and transferred to PVDF Hybond-p membranes (GE Healthcare, Milano, Italy). Membranes were blocked with ECL-Blocking Solution (GE Healthcare, Milano, Italy) overnight, with rotation at 4 °C. Membranes were then incubated with primary antibodies against cyclin A (Upstate), cyclin B1 (BD), p53, Bcl-2, Bcl-XL, Bax, Cdc25c X-linked inhibitor of apoptosis protein (XIAP), PARP, procaspase-9, procaspase-8, procaspase-2, cleaved caspase-7, Akt, p-Akt^{Ser473}, mTOR, p-mTor^{Ser2448} (Cell Signaling, Milano, Italy), p21$^{cip1/waf1}$, β-actin (Sigma–Aldrich, Milano, Italy), and LC-3 (Novus Biologicals, Milano, Italy) overnight. Membranes were next incubated with peroxidase-conjugated secondary antibodies for 60 min. All membranes were visualized using ECL Advance (GE Healthcare, Milano, Italy) and exposed to Hyperfilm MP (GE Healthcare, Milano, Italy). To ensure equal protein loading, each membrane was stripped and reprobed with anti-β-actin antibody.

2.15. Plasmids and transfection

Myristoylated Akt (Myr-Akt) plasmid was purchased from Addgene (Cambridge, MA, USA). Cells were seeded into 6 well-plates the day before transfection. Transfection of Myr-Akt was performed with Effectene Transfection Reagent (Qiagen, Milano, Italy) according to the manufacturer's protocol.

2.16. Statistical analysis

Unless indicated otherwise, results are presented as mean ± SEM. The differences between different treatments were analyzed using the two-sided Student's *t* test. *p* values lower than 0.05 were considered significant

3. Results

3.1. MG-2477 binds to the colchicine site of tubulin and inhibits the polymerization of tubulin into microtubules

To evaluate if MG-2477 interfered with the microtubule network, we first examined its effects on cultured cells by immunofluorescence microscopy. Shown in Fig. 1, Panel B, is

the normal microtubule network of untreated cells. Following 24 h of treatment with MG-2477 at 1.0 μM, there was extensive disruption of the microtubule network. Treated cells showed a characteristic “rounded up” morphology caused by loss of microtubules in both interphase and mitotic cells. We also examined cells for arrest in mitosis following treatment with MG-2477 (Fig. 1, Panel C). Large numbers of cells arrested in metaphase were apparent from their condensed chromosomes and lost nuclear membrane. The percentage of mitotic cells (the mitotic index) increased in a concentration dependent manner following treatment with MG-2477.

These cellular effects implied that MG-2477 interfered with tubulin polymerization. We therefore examined its effects on the assembly of purified tubulin [19]. We added different concentrations of MG-2477 to 10 μM αβ-tubulin and compared its effects with those of two reference compounds, combretastatin A-4 (CA4) and thiocolchicine. MG-2477 inhibited tubulin polymerization with an IC_{50} value of 0.9 μM (Fig. 2, Panel A), a value lower than that of CA4 (IC_{50}, 1.2 μM) but similar to that of thiocolchicine (IC_{50}, 0.8 μM).

To determine if MG-2477 interacted with tubulin at the colchicine site, we determined whether it inhibited binding of 5 μM [^{3}H]colchicine to 1 μM tubulin, again in comparison with CA4 and thiocolchicine. The inhibitors were used at both 1 and 5 μM. MG-2477 significantly inhibited [^{3}H]colchicine binding to tubulin, indicating that it acts at the colchicine site. Its inhibitory effect, however, was lower than that of CA4 but greater than that of thiocolchicine (Fig. 2, Panel B).

The 1SA0 tubulin structure [21] was used for computer-based automated docking of MG-2477 in comparison with colchicine. This was performed using the MOE-Dock program. Fig. 2 (Panel C) depicts the binding mode of MG-2477 in the colchicine site. The colchicine site is largely buried in the intermediate domain of the β-subunit, although colchicine also interacts with loop T5 of the neighboring α-subunit (Fig. 2, Panel C), consistent with the observation that colchicine stabilizes the tubulin heterodimer [21]. Docking simulations showed that, like colchicine, MG-2477 can be accommodated in the same hydrophobic cleft, adopting an energetically stable conformation. Moreover, the most stable conformation of MG-2477 displayed the same chemical interactions as colchicine, predominantly hydrophobic interactions with Val 181, Ala 250, Cys 241, Val 318, and Ile 378. Again, like colchicine, MG-2477 interacted with the neighboring α-tubulin T5 loop, consistent with a competitive mechanism of action at the colchicine site.

3.2. MG-2477 induces cell cycle arrest at the G2/M phase of the cell cycle

The effect of MG-2477 on cell cycle progression was examined by flow cytometry. MG-2477 treatment resulted in the accumulation of cells in the G2/M phase, with a concomitant reduction in the proportion of cells in the G1 phase. A small decrease of cells in the S phase was also observed (Fig. 3, Panels A and B). The accumulation in G2/M cells began after 12 h of treatment and is concentration dependent until the concentration of 0.25 μM, after which a plateau was reached. The characteristic hypodipolid peak (subG1), indicating apoptotic cells, did not appear until after 48 h of treatment (Fig. 3, Panel C).

Next, we investigated the association between MG-2477-induced G2/M arrest and alterations in G2/M regulatory protein expression. As shown in Fig. 3 (Panel D), MG-2477 caused an increase in cyclin B1 expression after 12 and 24 h, followed by a decrease at 48 h. Similar effects occurred in the expression of cyclin A. At 24 h, a slower migrating form of phosphatase Cdc25c appeared, indicating changes in the phosphorylation status of this protein. As early as 12 h, increased levels of p53 protein were expressed in response to treatment with MG-2477, but there was little change in expression of $p21^{waf/Cip1}$.

3.3. MG-2477 induces growth inhibition and delayed apoptotic response in A549 cells

A549 cells exposed to 1 μM MG-2477 were analyzed for viability at 24, 48 and 72 h by the MTT assay. Cells exhibited a lag period lasting over 24 h in their response to MG-2477, while a significant decrease in viability occurred at 48 and 72 h (Fig. 4, Panel A).

To characterize the mode of cell death, we performed a biparametric cytofluorimetric analysis using PI and Annexin-V-FITC, which stain DNA and PS residues, respectively [28]. After drug treatment for 12, 24 or 48 h, A549 cells were labeled with the two dyes and washed, and the resulting red (PI) and green (FITC) fluorescence was monitored by flow cytometry. We observed the appearance of Annexin-V^+/PI^- cells, indicative of apoptosis, as shown in the representative histograms depicted in Fig. 4 (Panel B, upper). Quantitatively, MG-2477 treatment resulted in a significant induction of apoptotic cells only after 48 h of treatment (Fig. 4, Panel B, lower), consistent with the appearance of subG1 cells described above.

It is well established that, at an early stage, apoptotic stimuli alter the mitochondrial transmembrane potential ($\Delta\psi_{mt}$) [29,30]. To address whether MG-2477 affected the $\Delta\psi_{mt}$, we examined treated cells for fluorescence of the dye JC-1. No significant changes in mitochondrial potential were observed (Fig. 4, Panel C). To confirm that mitochondria were not involved in the mechanism of apoptosis, we also evaluated the mitochondrial production of ROS by two fluorescent probes, HE and H_2DCFDA, using flow cytometry. In agreement with the low levels of mitochondrial depolarization, only a slight increase of ROS production was observed in cells treated with MG-2477 (Fig. 4, Panel C). Furthermore, immunofluorescence and flow cytometric analysis of cells treated with the compound did not show any release of cytochrome *c* (Fig. 4, Panels D and E), indicating that the late apoptosis induced by MG-2477 did not follow a mitochondrial pathway.

The activation of caspases plays a central role in the process of apoptotic cell death [31]. We therefore wondered whether inhibition of caspases with the pan-caspase inhibitor z-VAD.fmk would prevent cell death. Our results showed that z-VAD.fmk significantly reduced cell mortality as assessed by flow cytometry after double staining with PI and Annexin-V (Fig. 5, Panel A), indicating that cell death induced by MG-2477 is caspase-dependent.

To determine which caspases were involved in MG-2477-induced cell death, the expression of caspases was measured by immunoblot analysis and flow cytometry. We observed a clear activation of two effector caspases, caspase-7 and caspase-3, and we also observed cleavage of the caspase-3 substrate PARP after 48 h of MG-2477 exposure (Fig. 5, Panels B and C). In addition, the expression of XIAP, a member of the inhibitors of apoptosis protein family, was strongly reduced concomitant with caspase activation. Consistent with the $\Delta\psi_{mt}$ results described above, MG-2477 treatment did not induce activation of caspase-9, the major initiator caspase of the intrinsic (mitochondrial) apoptosis pathway, nor of caspase-8. As shown in Fig. 5, Panel C, expressed levels of these proteins did not change significantly following treatment with MG-2477. Caspase-2 is a unique caspase with characteristics of both initiator and effector caspases [32]. Recently, its key role in several apoptosis signaling cascades has emerged. In particular, caspase-2 has been implicated in the cell death induced by different antimitotic agents [33,34]. Western blot analysis showed an early activation of caspase-2 following treatment with MG-2477 that occurred prior to caspase-3/7 activation (Fig. 5, Panel C). In agreement with these data, the caspase-9 inhibitor z-LEDH.fmk did not prevent apoptosis, while the selective caspase-2 inhibitor z-VDVAD.fmk, significantly reduced cell death induced by MG-2477 (Fig. 5, Panel A).

3.4. Effect of MG-2477 on Bcl-2 family proteins

There is increasing evidence that regulation of the Bcl-2 family of protein shares the signaling pathways induced by antimicrotubule compounds [4]. Our results showed (Fig. 6, Panel A) that the anti-apoptotic proteins Bcl-2 and Bcl-XL were phosphorylated in the first 12–24 h of treatment, as demonstrated by band shifts, followed by reduction in expression of the proteins at 48 h. Mcl-1, an anti-apoptotic member of the Bcl-2 family, was also phosphorylated in response to MG-2477 treatment. The Mcl-1 band then disappeared at 48 h with the occurrence of apoptosis, following treatment with 1 μM MG-2477. MG-2477 treatment had little or no effect on the expression of proapoptotic proteins such as Bax or Bak (Fig. 6, Panel B).

3.5. MG-2477 induces autophagy in A549 cells

In view of the minimal level of apoptosis observed following 12–24 h of treatment with MG-2477, we examined whether autophagy was induced in A549 cells with MG-2477 treatment. We first examined levels of LC3-II induced by MG-2477 treatment, since this protein is a good indicator of autophagosome formation [35]. As shown in Fig. 7 (Panel A), MG-2477 induced, in a time-dependent manner, an increase in the amount of LC3-II. This effect was already evident after 12 h of treatment, in contrast to the low levels of apoptosis at this time point. We next used monodansylcadaverine, a dye that stains autophagosomes [35]. As shown in Fig. 7 (Panel B), MDC-positive vacuoles were detected after MG-2477 treatment.

A typical characteristic of autophagy is the development of AVOs [10]. Observations with fluorescence microscopy of A549 cell treated with MG-2477 and stained with the fluorescent probe AO showed an increase in cell size and cytoplasmic acidic vacuolization, as shown in Fig. 7 (Panel B). To quantify the appearance of AVOs after treatment with MG-2477, we performed flow cytometric analysis after staining of the cells with AO. In good agreement with the early appearance of LC3-II, there was also a significant increase in red fluorescence after 24 h of treatment (Fig. 7, Panel C). A recent study [36] reports that vincristine disruption of the microtubule cytoskeleton may interfere with the fusion of autophagosomes with lysosomes. We therefore visualized autophagosome formation in A549 cells by using a cell line expressing the autophagosome-associated LC3 protein fused to green fluorescent protein (GFP-LC3). MG-2477 induced a redistribution of GFP-LC3 from a diffuse to a vacuolar pattern when autophagosomes were formed (Fig. 7, Panel D). More importantly, these autophagosomes co-localized with the lysosomotropic dye LysoTracker RED, indicating the effective formation of autophagolysosomes.

3.6. Inhibition of autophagy potentiates MG-2477-induced apoptotic cell death

To investigate whether inhibition of autophagy would affect the cytotoxicity of MG-2477, A549 cells were treated with 1 μM MG-2477 in the presence of 3-MA or bafilomycin A1, two well known inhibitors of autophagy [37,38]. As shown in Fig. 8 (Panel A), the presence of bafilomycin A1 or 3-MA significantly increased the percentage of apoptotic cells as detected by the Annexin-V assay. Furthermore, the activation of caspase-3 was also enhanced in the presence of either 3-MA or bafilomycin A1 (Fig. 8, Panel B). Importantly, to explore the role of mitochondria when autophagy was inhibited, we analyzed the mitochondrial potential and the activation of caspase-9 in the presence of 3-MA and bafilomycin A1. We did not observe significant variations with respect to the cells treated in the absence of the two inhibitors either of the mitochondrial depolarization (Fig. 8, panel C) or of caspase-9 activation (Fig. 8, Panel D). In contrast, a potentiation of caspase-2 was observed after treatment of the cells with MG-2477 in the presence of either of the autophagy inhibitors (Fig. 8, Panel D).

3.7. MG-2477 induces inhibition of the PI3K/Akt/mTOR pathway

PI3K/Akt/mTOR signaling is one of the major pathways activated in cancer cells, including lung cancer cells. This pathway plays a variety of physiological roles, including regulation of cell growth, of the cell cycle and of cell survival. Recent studies have indicated that inhibition of the PI3K/Akt/mTOR pathway is associated with triggering autophagy in cancer cells [15,16].

As shown in Fig. 9 (Panel A), treatment with MG-2477 reduced the expression of p85, the regulatory subunit of PI3K after 24 h of treatment and, at the same time, caused a decrease in the phosphorylation (at Ser^{473}) of the Akt protein. Similar responses were observed for the phosphorylated forms of the Akt downstream protein FKHR (Ser^{256}).

We further investigated the effect of MG-2477 treatment on mTOR activity. Exposure of A549 cells to MG-2477 resulted in diminished levels of the phosphorylated (activated) form of mTOR (Ser^{2448}), while total mTOR levels were not affected by the treatment. MG-2477 treatment also induced a sharp decrease in the phosphorylation of the mTOR targets p70 ribosomal protein S6 kinase and 4E-BP1, revealing a potent inhibitory effect of MG-2477 treatment on Akt/mTOR signaling.

To evaluate the relationship between MG-2477-induced autophagy and the Akt pathway, we transiently transfected A549 cells with a Myr-Akt plasmid, coding for an active form of Akt. Compared with the control cells, in cells transfected with the vector plasmid the expression of Akt was dramatically increased (Fig. 9, Panel B, upper). Then we evaluated the effects of MG-2477 treatment on these cells. As shown in Fig. 9 (Panel C), cells overexpressing Akt were refractory to MG-2477-induced autophagy as compared with cells transfected with the empty vector. The cells overexpressing Akt and treated with MG-2477 showed a significant reduction in LC3-II expression (Fig. 9, Panel B, lower) and in formation of AVOs (Fig. 9, Panel C). In addition, no significant variation in cell viability was observed in the Akt overexpressing cells (Fig. 9, Panel D), in good agreement with the data reported by Vanderweele et al. [39] and Asnaghi et al. [40], which showed that Akt up-regulation promotes a selective resistance to different antimicrotubule agents but not other chemotherapic drugs.

4. Discussion

Previous studies demonstrated that MG-2477 displayed effective antiproliferative activity in numerous cell lines derived from human solid tumors, including multidrug resistant cell lines [17]. In this study we showed that MG-2477 induced depolymerization of tubulin and inhibited normal spindle formation in A549 cells, resulting in mitotic arrest and cell death. The inhibition of tubulin polymerization was similar to that observed with reference compounds such as CA4. Examination of the effects of MG-2477 on [^{3}H]colchicine binding to tubulin revealed that colchicine binding was efficiently inhibited, indicating that MG-2477 binds in the colchicine site. These data were supported by molecular docking analysis.

From this point of view of the cytotoxic mechanism of action of MG-2477, we provided evidence that the compound induced autophagy in A549 cells, followed by apoptotic cell death. Autophagy was morphologically and biochemically characterized, including the appearance in treated A549 cells expressing GFP-LC3 of cytoplasmic vacuoles that displayed punctuate fluorescence indicative of LC3 recruitment to the autophagosome.

Our results showed that MG-2477 treatment decreased the expression of the PI3K p85 regulatory subunit, followed by Akt dephosphorylation on Ser^{473}. The inhibitory effects of

MG-2477 on PI3K/Akt were correlated with the dephosphorylation of FKHR, an Akt downstream protein target. Moreover, exposure of cells to MG-2477 also inactivated mTOR and reduced phosphorylation of its downstream targets p706K and 4E-BP1. Thus, these results are consistent with many recent studies indicating that inhibition of the Akt/mTOR pathway is associated with induction of autophagy in cancer cells [16,41,42].

At present, the precise molecular mechanism that switches between autophagy and apoptosis is not clear. Autophagy and apoptosis can be induced in response to different cellular stresses, and the induction of autophagy/apoptosis can occur sequentially, simultaneously or in a mutually exclusive manner [43]. Our observations indicate that pharmacological inhibition of autophagy with 3-MA or bafilomycin A1 does not activate, but only enhances, apoptotic death, suggesting that autophagy induced by MG-2477 is an adaptive response in A549 cells.

It has been suggested that microtubules are essential for the endocytic and autophagic pathways of membrane trafficking and facilitate autophagosome formation and serve to direct mature autophagosomes for degradation in lysosomes. [44]. However, a number of studies have shown that in mammalian cells, the disruption of the microtubule network provokes a delay in autophagy rather than a complete block of this process [45–47]. In particular, Köchl et al. [47] demonstrated this in rat hepatocytes expressing green fluorescent protein (GFP)-LC3. When these cells were pre-treated with the antimitotic agents nocodazole and vinblastine, prior to inducing autophagy, the formation of autophagosomes was facilitated by but did not require microtubules. Moreover, analysis of LC3-II turnover and of the overlap of GFP-LC3-positive vesicles with LysoTracker RED-positive lysosomes confirmed that intact microtubules contributed to the fusion of autophagosomes with lysosomes.

Our results are in good agreement with those of Köchl et al. [47] since we also showed a co-localization between GFP-LC3 autophagosomes and Lysotracker-positive vesicles that occurred following treatment with MG-2477, suggesting an accumulation of autophagolysosomes. Thus our data indicated that intact microtubules are not essential for targeting and for fusion with lysosomes.

Furthermore, our data indicated that cell death following MG-2477 treatment is caspase-dependent, as demonstrated by a significant increase in cell viability in the presence of the pan-caspase inhibitor z-VAD.fmk. Some studies, using different drugs, report that autophagy may precede mitochondrial-activated apoptosis [9,48]. An unexpected finding in our study was that mitochondrial functions such as mitochondrial polarization and release of cytochrome *c* were only slightly affected by treatment with MG-2477. This suggested that with MG-2477 treatment mitochondria were not involved in the cell death process. Of note, MG-2477 treatment did not induce activation of caspase-9, one of the major initiator caspases in the mitochondrial apoptosis pathway. Interestingly, caspase-2 seemed to be activated prior to caspase-3 and caspase-7, and the prevention of cell death induced by the selective caspase-2 inhibitor z-VDVAD.fmk indicated the major role played by this caspase. Newer evidence about the functions and activation mechanisms involved in apoptosis indicate that caspase-2 is unique among the caspases, displaying features of both initiator and executioner. Moreover, many recent studies indicate that activation of caspase-2 is fundamental for the induction of apoptosis induced by antimitotic drugs [33,34].

Several lines of evidence suggest that Bcl-2 phosphorylation is associated with the loss of antiapoptotic functions, although, in contrast, many other studies show that Bcl-2 is only a biochemical marker of G2/M phase events [4]. In addition, modulation of Bcl-2 expression can affect the induction of autophagy [49,50]. Our results showed that Bcl-2 is

phosphorylated in A549 cells treated with MG-2477 at early time points when hallmarks of apoptosis were not yet evident.

Asnaghi et al. [40] showed that Bcl-2 phosphorylation by antimitotic drugs is regulated by Akt and mTOR. They demonstrated this phenomenon by inhibiting mTOR signaling by inducing the expression of a dominant negative mutant of the Akt kinase in HEK293 cells. The levels of Bcl-2 phosphorylation after nocodazole treatment were higher in comparison with cells transfected with the empty vector. Interestingly, sensitivity to nocodazole was also significant increased. Opposite findings were obtained in HEK293 cells expressing constitutively active Akt. Thus, these results suggest that the level of activity of Akt may regulate Bcl-2 phosphorylation and the apoptotic threshold through the mTOR kinase. Other studies showed that, in cells where Akt is constitutively activated, the cytotoxic effects of different antimicrotubule agents are reduced [39,51]. However, the effects of these compounds are enhanced when a specific blockade of the Akt signaling pathway is produced. In our study, we did not observe any increase in MG-2477 induced cell death in A549 cells transiently transfected with a constitutively active form of Akt (Myr-Akt), but, at the same time, the cells were considerably more resistant to MG-2477 induced autophagy than cells transfected with the empty vector. Thus, these results strongly indicate that MG-2477-induced autophagy could be mediated by a block of the Akt pathway. In summary, the findings presented here indicate that MG-2477 is highly effective in reducing cell viability and that the reduced survival of A549 cells is associated with an initial autophagy that may be mediated by inhibition of the Akt/mTOR pathway. Autophagy is not the major cause of cell death but represents an adaptive early response to cellular stress that could enhance cell survival by retarding apoptosis. These results indicate that inhibition of autophagy might increase the efficacy of MG-2477 and that it could be a potential strategy for enhancing the chemotherapeutic effects of this compound.

References

1. Hadfield JA, Ducki S, Hirst N, McGrow AT. Tubulin and microtubules as targets for anticancer drugs. Prog Cell Cyc Res. 2003; 5:309–25.
2. Jordan MA, Wilson L. Microtubules as a target for anticancer drugs. Nat Rev Cancer. 2004; 4:253–65. [PubMed: 15057285]
3. Dumontet C, Jordan MA. Microtubule-binding agents: a dynamic field of cancer therapeutics. Nat Rev Drug Discov. 2010; 9:790–803. [PubMed: 20885410]
4. Mollinedo F, Gajate C. Microtubules, microtubule-interfering agents and apoptosis. Apoptosis. 2003; 8:413–50. [PubMed: 12975575]
5. Klionsky DJ. Autophagy: from phenomenology to molecular understanding in less than a decade. Nat Rev Mol Cell Biol. 2007; 8:931–7. [PubMed: 17712358]
6. Rubinsztein DC, Gestwicki JE, Murphy LO, Klionsky DJ. Potential therapeutic applications of autophagy. Nat Rev Drug Discov. 2007; 6:304–12. [PubMed: 17396135]
7. Kanzawa T, Germano IM, Komata T, Ito H, Kondo Y, Kondo S. Role of autophagy in temozolomide-induced cytotoxicity for malignant glioma cells. Cell Death Differ. 2004; 11:448–57. [PubMed: 14713959]
8. Laane E, Tamm Pokrovskaja K, Buentke Ito K, Kharazina P, Oscarsson J, et al. Cell death induced by dexamethasone in lymphoid leukemia is mediated through initiation of autophagy. Cell Death Differ. 2009:1018–29. [PubMed: 19390558]
9. Abedin MJ, Wang D, McDonnell MA, Lehmann U, Kelekar A. Autophagy delays apoptotic death in breast cancer cells following DNA damage. Cell Death Differ. 2007; 14:500–10. [PubMed: 16990848]
10. Paglin S, Hollister T, Delohery T, Hackett N, McMahill M, Sphicas E, et al. A novel response of cancer cells to radiation involves autophagy and formation of acidic vesicles. Cancer Res. 2001; 61:439–44. [PubMed: 11212227]

11. Zeng X, Kinsella TJ. Mammalian target of rapamycin and S6 kinase 1 positively regulate 6-thioguanine-induced autophagy. Cancer Res. 2008; 68:2384–9. [PubMed: 18381446]
12. Arthur CR, Gupton JT, Kellogg GE, Yeudall WA, Cabot MC, Newsham IF, et al. Autophagic cell death, polyploidy and senescence induced in breast tumor cells by the substituted pyrrole JG-03-14, a novel microtubule poison. Biochem Pharmacol. 2007; 74:981–91. [PubMed: 17692290]
13. Eum KH, Lee M. Crosstalk between autophagy and apoptosis in the regulation of paclitaxel-induced cell death in v-Ha-ras-transformed fibroblasts. Mol Cell Biochem. 2011; 348:61–8. [PubMed: 21069434]
14. Karna P, Zughaier S, Pannu V, Simmons R, Narayan S, Aneja R. Induction of reactive oxygen species-mediated autophagy by a novel microtubule-modulating agent. J Biol Chem. 2010; 285:18737–48. [PubMed: 20404319]
15. Guertin DA, Sabatini DM. Defining the role of mTOR in cancer. Cancer Cell. 2007; 1:9–22. [PubMed: 17613433]
16. Takeuchi H, Kondo Y, Fujiwara K, Kanzawa T, Aoki H, Mills GB, et al. Synergistic augmentation of rapamycin-induced autophagy in malignant glioma cells by phosphatydilinoditol 3-kinase/protein kinase B inhibitors. Cancer Res. 2005; 65:3336–46. [PubMed: 15833867]
17. Gasparotto V, Castagliuolo I, Ferlin MG. 3-substituted 7-phenyl-pyrroloquinolinones show potent cytotoxic activity in human cancer cell lines. J Med Chem. 2007; 50:5509–13. [PubMed: 17915851]
18. Viola G, Fortunato E, Cecconet L, Del Giudice L, Dall'Acqua F, Basso G. Central role of mitochondria and p53 in PUVA-induced apoptosis in human keratinocytes cell line NCTC-2544. Toxicol Appl Pharmacol. 2008; 227:84–96. [PubMed: 18048073]
19. Hamel E. Evaluation of antimitotic agents by quantitative comparisons of their effects on the polymerization of purified tubulin. Cell Biochem Biophys. 2003; 38:1–22. [PubMed: 12663938]
20. Verdier-Pinard P, Lai J-Y, Yoo H-D, Yu J, Marquez B, Nagle DG, et al. Structure-activity analysis of the interaction of curacin A, the potent colchicine site antimitotic agent with tubulin and effects of analogs on the growth of MCF-7 breast cancer cells. Mol Pharmacol. 1998; 53:62–76. [PubMed: 9443933]
21. Ravelli RB, Gigant B, Curmi PA, Jourdain I, Lachkar S, Sobel A, et al. Insight into tubulin regulation from a complex with colchicine and a stathmin-like domain. Nature. 2004; 428:198–202. [PubMed: 15014504]
22. MOE (Molecular Operating Environment), version 2008.10. Chemical Computing Group Inc; 1010 Sherbrooke Street West, Suite 910, Montreal, Quebec, Canada H3A 2R7: software available fromhttp://www.chemcomp.com
23. Baxter CA, Murray CW, Clark DE, Westhead DR, Eldridge MD. Flexible docking using tabù search and an empirical estimate of binding affinity. Proteins Struct Funct Genet. 1998; 33:367–82. [PubMed: 9829696]
24. Halgren T. Merck Molecular Force Field. I. Basis, form, scope, parameterization, and performance of MMFF94. J Comput Chem. 1996; 17:490–519.
25. Stewart, JJP. MOPAC. Vol. 7. Tokyo, Japan: Fujitsu Limited; 1993.
26. Wojciechowski M, Lesyng B. Generalized Born Model: analysis, refinement and applications to proteins. J Phys Chem B. 2004; 108:18368–76.
27. Pistollato F, Abbadi S, Rampazzo E, Viola G, Della Puppa A, Cavallini L, et al. Succinate and hypoxia antagonizes 2-deoxyglucose effects on glioblastoma. Biochem Pharm. 2010; 80:1517–27. [PubMed: 20705058]
28. Vermes I, Haanen C, Steffens-Nakken H, Reutelingsperger C. A novel assay for apoptosis. flow cytometric detection of phosphatidylserine expression on early apoptotic cells using fluorescein labelled Annexin V. J Immunol Methods. 1995; 184:39–51. [PubMed: 7622868]
29. Ly JD, Grubb DR, Lawen A. The mitochondrial membrane potential ($\Delta\psi_m$) in apotosis. Apoptosis. 2003; 3:115–28. [PubMed: 12766472]
30. Green DR, Kroemer G. The pathophysiology of mitochondrial cell death. Science. 2005; 305:626–9. [PubMed: 15286356]

31. Kumar S. Caspase function in programmed cell death. Cell Death Differ. 2007; 14:32–43. [PubMed: 17082813]
32. Vakifahmetoglu-Norberg H, Zhivotovsky B. The unpredictable caspase-2: what can it do? Trends Cell Biol. 2010; 20:150–9. [PubMed: 20061149]
33. Mhaidat NM, Wang Y, Kiejda KA, Zang XD, Hersey P. Docetaxel-induced apoptosis in melanoma cells is dependent on activation of caspase-2. Mol Cancer Ther. 2007; 6:752–61. [PubMed: 17308071]
34. Ho LH, Read SH, Dorstyn L, Lambrusco L, Kumar S. Caspase-2 is required for cell death induced by cytoskeletal disruption. Oncogene. 2008; 27:3393–404. [PubMed: 18193089]
35. Klionsky DJ, Abeliovich H, Agostinis P, Agrawal DK, Allev G, Askew DS, et al. Guidelines for the use and interpretation of assay for monitoring autophagy in higher eukaryotes. Autophagy. 2008; 4:151–75. [PubMed: 18188003]
36. Groth-Pedersen L, Ostenfeld MS, Hoyer-Hansen M, Nylandsted J, Jaattela M. Vincristine induces dramatic lysosomal changes and sensitizes cancer cells to lysosome-destabilizing siramesine. Cancer Res. 2007; 67:2217–25. [PubMed: 17332352]
37. Boya P, Gonzalez-Polo RA, Casares N, Perfettini JL, Dessen P, Metiver D, et al. Inhibition of macroautophagy triggers apoptosis. Mol Cell Biol. 2005; 25:1025–40. [PubMed: 15657430]
38. Gonzalez-Polo RA, Boya P, Pauleau AL, Jalil A, Larochette N, Souquere S, et al. The apoptosis/autophagic paradox: autophagic vacuolisation before apoptotic cell death. J Cell Sci. 2005; 118:3091–102. [PubMed: 15985464]
39. VanderWeele DJ, Zhou R, Rudin CM. Akt up-regulation increases resistance to microtubule-directed chemotherapeutic agents through mammalian target of rapamycin. Mol Cancer Ther. 2004; 3:1605–13. [PubMed: 15634654]
40. Asnaghi L, Calastretti A, Bevilacqua A, D'Agnano I, Gatti G, Canti G, et al. Bcl-2 phosphorylation and apoptosis activated by damaged microtubules require mTOR and are regulated by Akt. Oncogene. 2004; 23:5781–91. [PubMed: 15208671]
41. Saiki S, Sasazawa Y, Imamichi Y, Kawajiri S, Fujimaki T, Tanida I. Caffeine induces apoptosis by enhancement of autophagy via PI3K/Akt/mTOR/p70S6K inhibition. Autophagy. 2011; 7:176–87. [PubMed: 21081844]
42. Degtyarev M, De Mazière A, Orr C, Lin J, Lee BB, Tien JY, et al. Akt inhibition promotes autophagy and sensitizes PTEN-null tumors to lysosomotropic agents. J Cell Biol. 2008; 183:101–16. [PubMed: 18838554]
43. Eisenberg-Lerner A, Bialik S, Simon HU, Kimchi A. Life and death partners: apoptosis, autophagy and the cross-talk between them. Cell Death Differ. 2009; 16:966–75. [PubMed: 19325568]
44. Monastyrska I, Rieter E, Klionsky DJ, Reggiori F. Multiple roles of the cytoskeleton in autophagy. Biol Rev. 2009; 84:431–48. [PubMed: 19659885]
45. Fass E, Shvets E, Degani I, Hirschberg K, Elazar Z. Microtubules support production of starvation-induced autophagosomes but not their targeting and fusion with lysosomes. J Biol Chem. 2006; 281:36303–16. [PubMed: 16963441]
46. Jahreiss L, Menzies FM, Rubinsztein DC. The itinerary of autophagosomes: from peripheral formation to kiss-and-run fusion with lysosomes. Traffic. 2008; 9:574–87. [PubMed: 18182013]
47. Köchl R, Hu XW, Chan EY, Tooze SA. Microtubules facilitate autophagosome formation and fusion of autophagosomes with endosomes. Traffic. 2006; 7:129–45. [PubMed: 16420522]
48. Sy LK, Yan SC, Lok CN, Man RYK, Che CM. Timosaponin AIII induces autophagy preceding mitochondria-mediated apoptosis in HeLa cancer cells. Cancer Res. 2008; 68:10229–37. [PubMed: 19074891]
49. Pettingre S, Tassa A, Qu X, Liang XH, Mizushima N, Packer M, et al. Bcl-2 antiapototic proteins inhibit Beclin 1-dependent autophagy. Cell. 2005; 122:927–39. [PubMed: 16179260]
50. Levine B, Sinha S, Kroemer G. Bcl-2 family members: dual regulator of apoptosis and autophagy. Autophagy. 2008; 4:600–6. [PubMed: 18497563]
51. Fuijiwara Y, Hosokawa Y, Watanabe K, Tanimura S, Ozaki K, Kohno M. Blockade of the phosphatidylinositol-3-kinase-Akt signaling pathway enhances the induction of apoptosis by microtubule-destabilizing agents in tumor cells in which the pathway is constitutively activated. Mol Cancer Ther. 2007; 6:1133–42. [PubMed: 17363506]

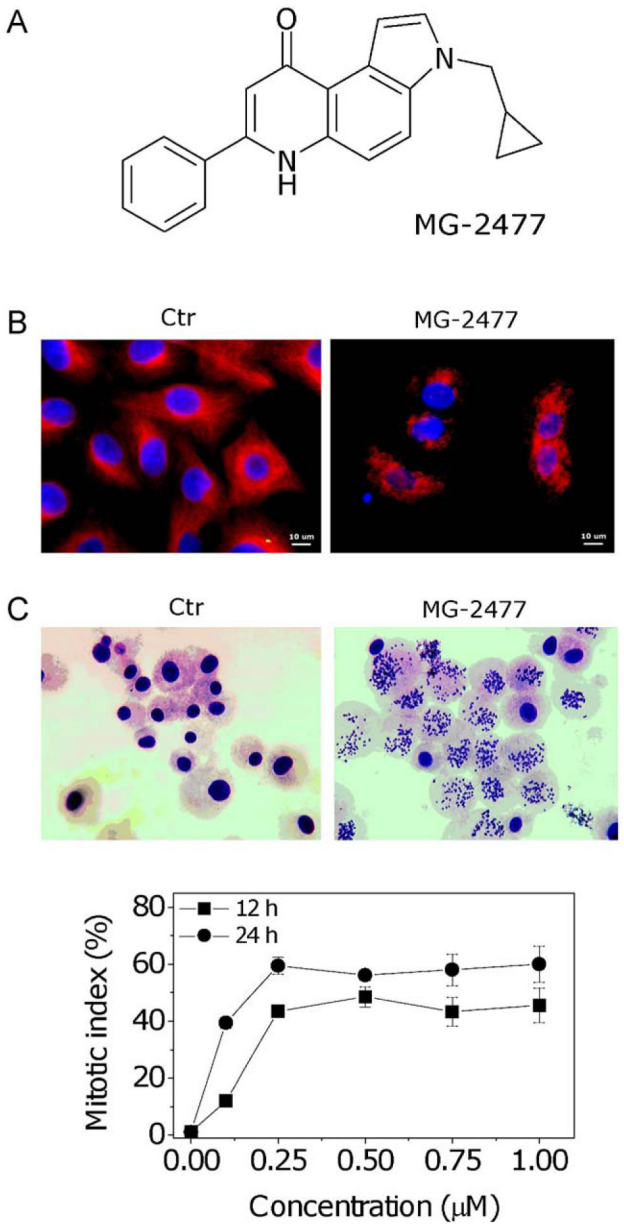

Fig. 1.

MG-2477 inhibits tubulin assembly and destabilizes microtubules by acting at the colchicine site of tubulin. (A) Chemical structure of MG-2477. (B) Immunofluorescence images of A549 cells treated with anti-β-tubulin antibody and with a TRITC-conjugated secondary antibody and then observed by confocal microscopy. Cells were either untreated or exposed to 1 μM MG-2477 for 24 h, as indicated. (C) Quantitative assessment of mitotic arrest by MG-2477. A549 cells were treated with the compound at the indicated concentrations. Two hundred cells/treatment were scored for the presence of mitotic figures by contrast phase microscopy, and the mitotic index was calculated as the proportion of cells with mitotic figures. Data are expressed as mean ± SEM of three independent experiments.

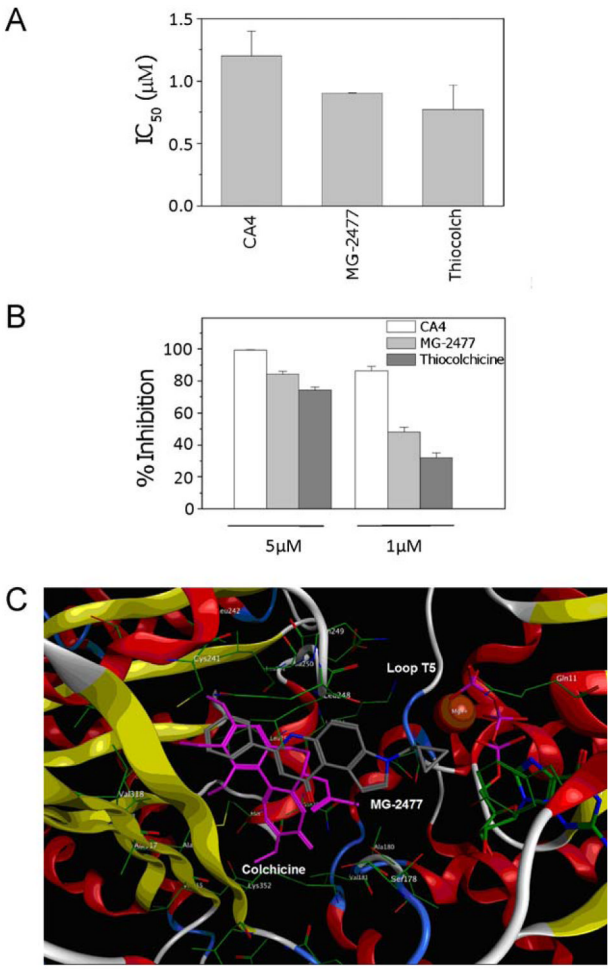

Fig. 2.

Inhibition of microtubule assembly and colchicine binding. (A) To evaluate the effect of the compound on tubulin assembly *in vitro*, varying concentrations of compound were preincubated with 10 μM bovine brain tubulin. Following addition of GTP, tubulin assembly at 30 °C was followed turbidimetrically at 350 nm. The IC_{50} was defined as the compound concentration that inhibited the extent of assembly by 50% after a 20 min incubation. (B) The capacity of the test compound to inhibit colchicine binding to tubulin was measured in reaction mixtures that contained 1 μM tubulin, 5 μM [^{3}H]colchicine and 1 or 5 μM MG-2477, as indicated. Thiocolchicine and CA4 were used as reference compounds. Data are expressed as mean ± SD of two independent experiments. (C) Docked pose of MG-2477 (gray), overlapped with colchicine (pink) in the tubulin binding site. (For interpretation of the references to color in this figure legend, the reader is referred to the web version of the article.)

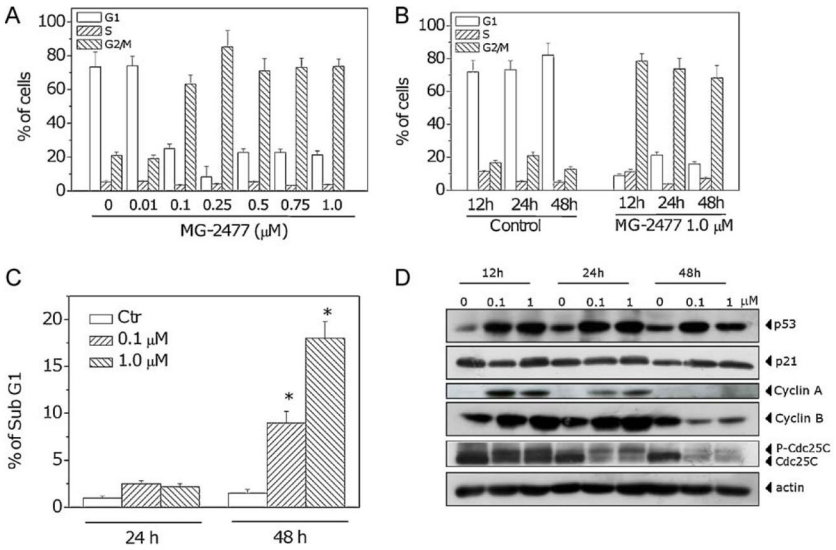

Fig. 3.

Effects of MG-2477-induced G2/M phase arrest in A549 cells. (A) Cells were treated with different concentrations of MG-2477 for 24 h, and cell cycle distribution was analyzed by flow cytometry after staining the cells with PI. (B) Cells were treated with 1 μM MG-2477 for the indicated times, and cell cycle distribution was analyzed as above. Data are expressed as mean ± SEM of three independent experiments. (C) Percentage of cells in the subG1 peak. Cells were treated with MG-2477 at 0.1 and 1.0 μM for 24 and 48 h. Data are expressed as mean ± SEM of three independent experiments. *$p < 0.01$ vs. control. (D) Cells were treated with the indicated concentration of MG-2477 for the indicated times. Whole cell lysates were subjected to Western blot analysis.

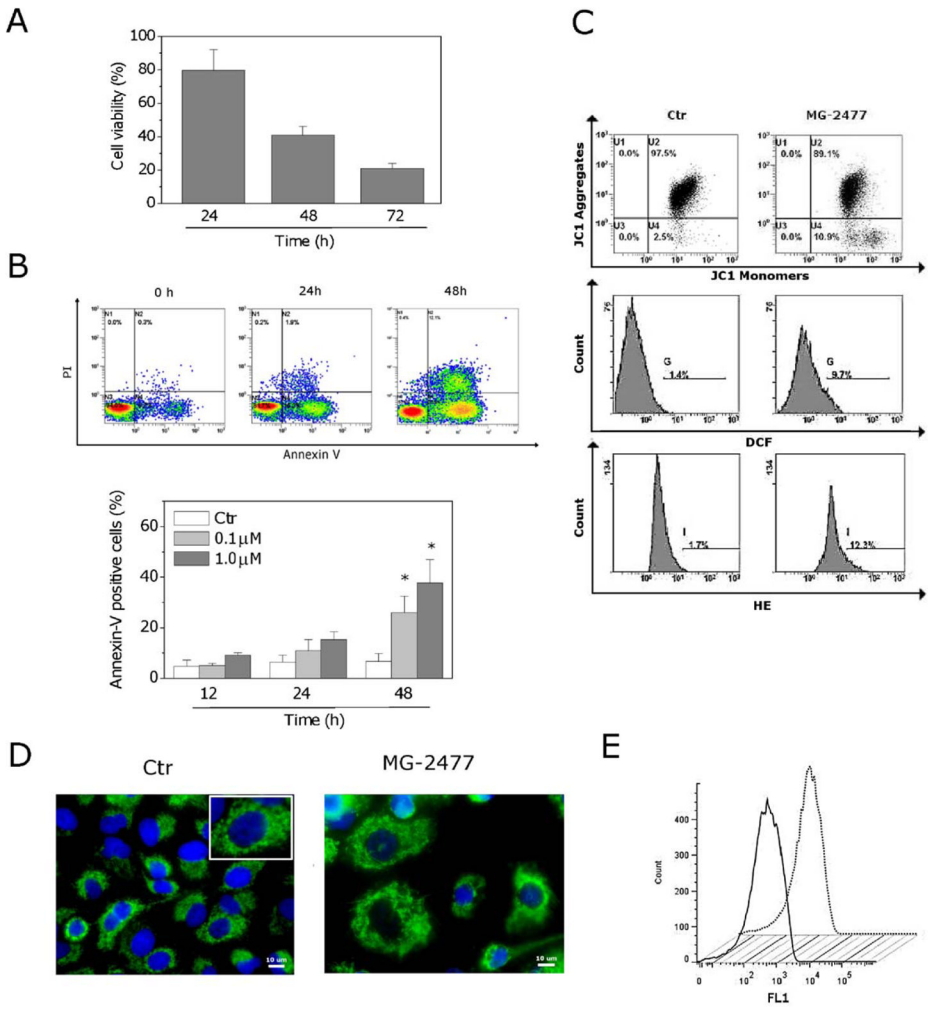

Fig. 4.

MG-2477 induced delayed apoptosis in A549 cells. (A) Cells were incubated with 1 μM MG-2477 for the indicated times. Cell viability was quantified by the MTT assay. (B) Representative histograms of A549 cells treated with MG-2477 (upper panel) and analyzed by flow cytometry after double staining of the cells with Annexin-V-FITC and PI (lower panel). Data are expressed as mean ± SEM of six independent experiments. *$p < 0.01$ vs. control. (C) Analysis of mitochondrial dysfunction in cells treated with 1 μM MG-2477 for 48 h and analyzed by flow cytometry for mitochondrial depolarization. Cells were labeled with the dye JC-1, which measures depolarization. ROS production was measured after labeling the cells with the fluorescent probes H_2DCFDA and HE. (D) Representative confocal images of control A549 cells and cells treated with 1 μM MG-2477 for 48 h, showing cytochrome *c* labeled with a monoclonal antibody conjugated to FITC. The nuclei were stained blue with DAPI. Scale bar, 10 μm. Inset in the control cells image: an enlargement of one cell for a better comparison with the treated cells. (E) Flow cytometric analysis of cytochrome *c* after treatment with MG-2477 (1 μM) for 48 h. Cells were stained with a FTIC-conjugated monoclonal antibody directed against cytochrome *c*. Straight line: control cells; dotted line: MG-2477 treated cells. (For interpretation of the references to color in this figure legend, the reader is referred to the web version of the article.)

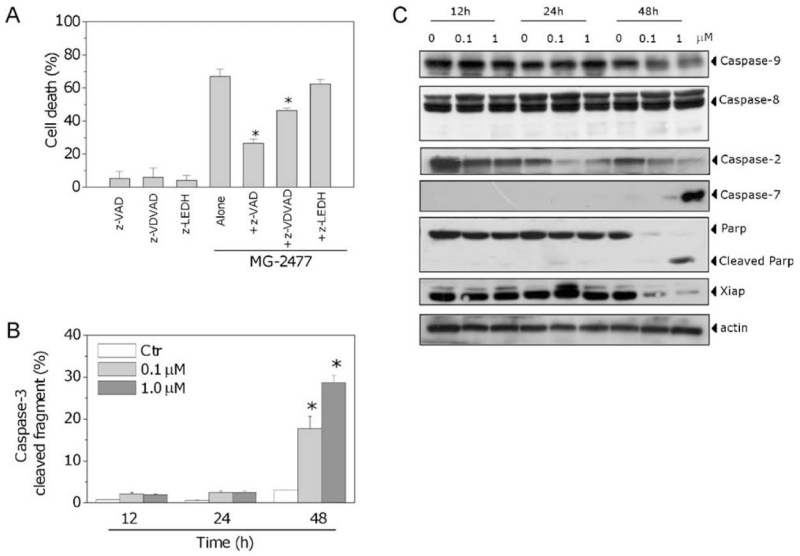

Fig. 5.

(A) Cells were incubated with 1 μM MG-2477 in the presence or absence of the pan-caspase inhibitor z-VAD.fmk (100 μM), the caspase-2 inhibitor z-VDVAD.fmk (100 μM), or the caspase-9 inhibitor z-LEDH.fmk (100 μM), for 48 h. Cell death was determined by flow cytometric analysis of Annexin-V and PI uptake. Mean ± SEM of three independent experiments. The asterisk indicates $p < 0.01$ vs. MG-2477 alone. (B) Activation of caspase-3 by MG-2477. Cells were treated with 0.1 or 1.0 μM MG-2477 for 24 or 48 h, harvested and stained with an anti-human active caspase-3 fragment monoclonal antibody conjugated to FITC. Data obtained by flow cytometric analysis is expressed as percentage of caspase-3 active fragment positive cells. Mean ± SEM of five independent experiments. *$p < 0.01$ vs. control. (C) Expression of caspases, PARP and XIAP following treatment with MG-2477, as indicated.

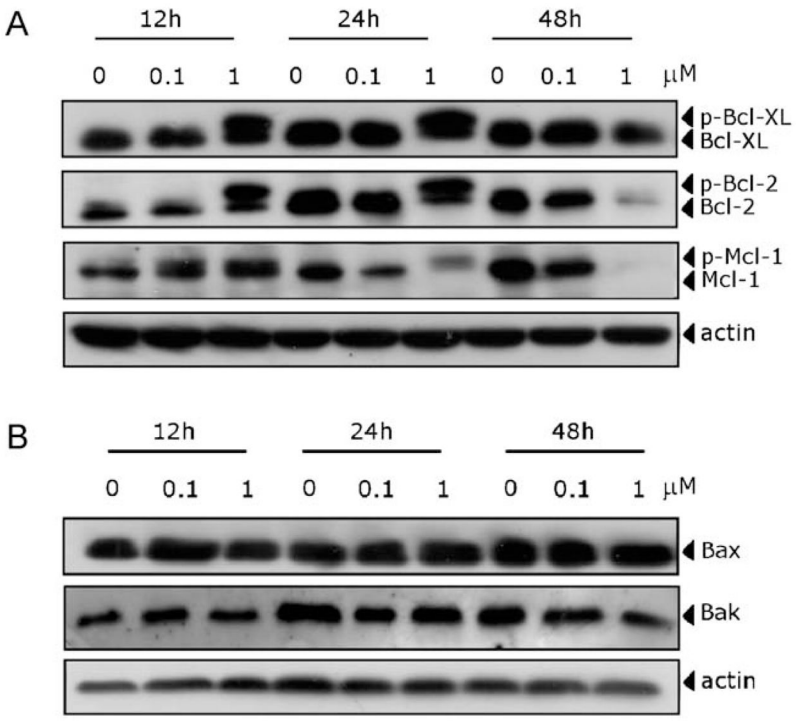

Fig. 6.

Effect of MG-2477 treatment, as indicated, on the expression of anti-apoptotic (A) and pro-apoptotic (B) member proteins of the Bcl-2 family.

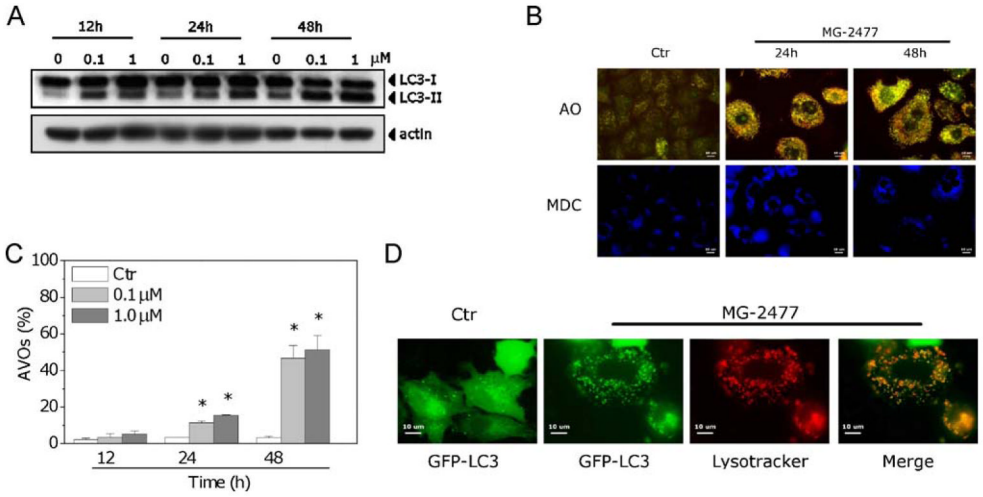

Fig. 7.

(A) Immunoblot analysis of LC3 after treatment with MG-2477, as indicated. (B) Fluorescence microscopic analysis of A549 cells treated with 1 μM MG-2477 for 24 or 48 h and then stained with AO or MDC, as indicated. (C) Detection of MG-2477-induced AVO formation in A549 cells. Cells were treated with MG-2477, as indicated, stained with AO and analyzed by flow cytometry. Mean ± SEM of four independent experiments. *$p < 0.01$ vs. non-treated cells. (D) A549 cells were transiently transfected with GFP-LC3 and treated with 1 μM MG-2477 for 24 h. Lysosomes were stained with LysoTracker RED, and cells were analyzed by confocal microscopy.

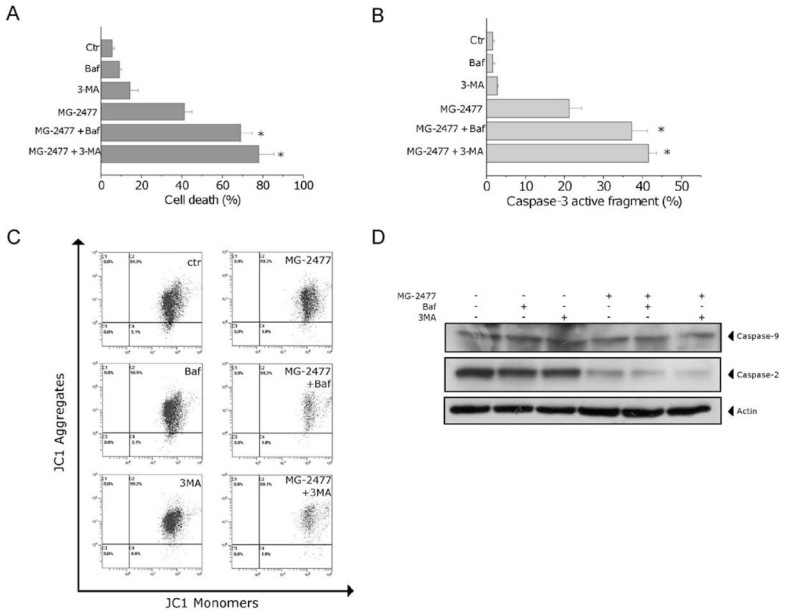

Fig. 8.

(A) Cells were incubated with 1 μM MG-2477 in the presence or absence of 3-MA (1 mM) or bafilomycin A1 (2 nM) for 48 h. Cell death was determined by flow cytometric analysis of Annexin-V and PI uptake. Mean ± SEM of three independent experiments. *$p < 0.01$ vs. MG-2477 alone. (B) Cells were incubated with 1 μM MG-2477 in the presence or absence of 3-MA (1 mM) or bafilomycin A1 (2 nM) for 48 h. Cells were stained with an anti-human active caspase-3 fragment monoclonal antibody conjugated to FITC. Data obtained by flow cytometric analysis is expressed as the percentage of caspase-3 active fragment positive cells. Mean ± SEM of three independent experiments. *$p < 0.01$ vs. MG-2477 alone. (C) Representative histograms of flow cytometric analysis of mitochondrial depolarization after treatment of A549 cells with MG-2477 (1 μM) for 48 h in the presence of 3-MA or bafilomycin A1. (D) Western blot analysis of procaspase-9 and procaspase-2 after 48 h of MG-2477 (1 μM) in the presence of 3-MA or bafilomycin A1, as indicated.

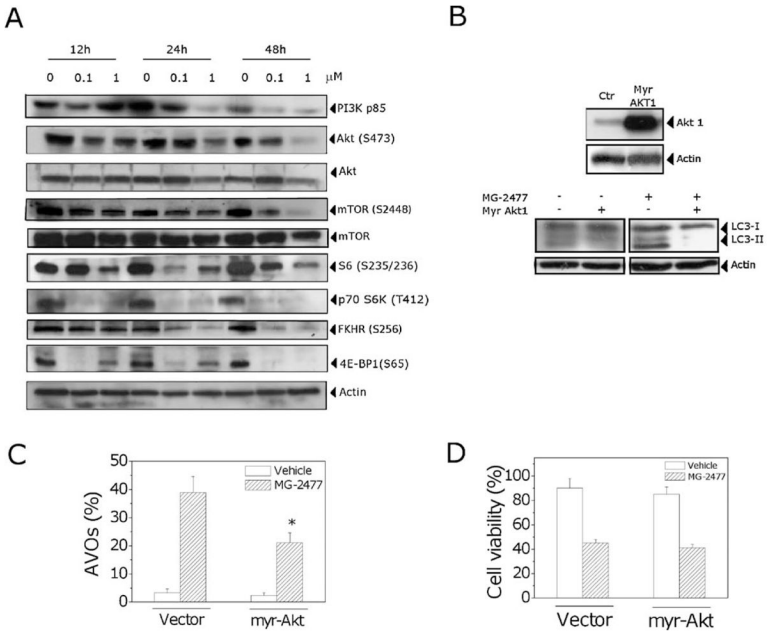

Fig. 9.

(A) Effect of MG-2477 treatment on the PI3K/Akt/mTOR pathway. Cells were treated with MG-2477, as indicated, harvested and subjected to Western blot analysis. (B) A549 cells overexpressing Akt after Myr-Akt transfection (upper). Immunoblot analysis of LC-3 in Myr-Akt transfected cells treated with MG-2477 (1 μM) (lower). (C) Detection of AVO formation in Myr-Akt transfected cells treated with 1 μM MG-2477. Cells were treated for 48 h, stained with AO and analyzed by flow cytometry. Mean ± SEM of three independent experiments. *$p < 0.01$ vs. the cells with the empty vector treated with MG-2477. (D) Percentage of viable cells in Myr-Akt transfected cells treated with MG-2477 (1 μM) for 48 h. Mean ± SEM of three independent experiments.